UDC: 536:546.231
ORCID: 0000-0001-5050-9858 (Ashirov)
ORCID: 0000-0002-3275-5833 (Babanly)
ORCID: 0000-0003-2357-6195 (Mashadiyeva)

THERMODYNAMIC STUDY OF SILVER-SILICON SELENIDES (TELLURIDES) BY THE EMF METHOD WITH AG_4RBI_5 SOLID ELECTROLYTE

Garay Mikayil Ashirov, Kamala Nagı Babanly, Leyla Farhad Mashadiyeva
Academician M.Nagiev named Catalysis and Inorganic Chemistry Institute of the Ministry of Science and Education
E-mail: garayasirov@gmail.com
Received: 04.04.2023
Accepted: 31.08.2023

The Ag_2Se-$SiSe_2$-Se subsystem of the Ag-Si-Se system was studied in the 360-450 K temperature range, while the Ag_2Te-Si_2Te_3-Te subsystem of the Ag-Si-Te system was studied in the 300-450 K temperature range by the EMF (Electromotive Force) method with Ag_4RbI_5 solid electrolyte. It was observed that the dependence of EMF on temperature was linear in the samples prepared for both systems. Partial thermodynamic functions of silver in alloys of Ag-Si-Se(Te) systems, as well as standard integral thermodynamic functions of ternary compounds Ag_8SiSe_6 and Ag_8SiTe_6 were calculated based on the results of EMF measurements. Besides, standard integral thermodynamic functions of β-Ag_8SiSe_6 were calculated both under standard conditions and at 400 K.

Keywords: *silver-silicon selenides, tellurides, phase transition, thermodynamic functions, EMF method, Ag_4RbI_5 solid electrolyte.*

DOI: https://doi.org/10.59849/2409-4838.2023.3.45

INTRODUCTION

Silver-containing ternary chalcogenides are considered valuable functional materials [1-3]. These compounds exhibit high photoelectric, optical, and thermoelectric properties and therefore are considered promising for use in alternative energy devices and various fields of modern electronics [4-17]. In addition, some of these compounds show ionic conductivity due to the mobility of Ag^+ cations and thus, can be used as electrochemical sensors, electrode materials, and batteries as well [18-21]. It is known that the search and study of new multicomponent materials are based on information about the phase equilibria and the thermodynamic properties of the corresponding systems [22-25]. The study of thermodynamic functions using EMF measurements is well-known and proven method. The discovery of unipolar superionic conductors with Ag^+ conductivity makes it possible to use these materials as solid electrolytes in electrochemical cells. Such electrochemical cells have already been successfully used in many works during thermodynamic studies of silver-based complex systems [26-35]. In this work, we report the results of a thermodynamic study of Ag_2Se-$SiSe_2$-Se and Ag_2Te-Si_2Te_3-Te subsystems using the EMF method with Ag_4RbI_5 solid electrolyte in the temperature range of 360-450 K and 300-450 K, respectively. Both Ag-Si-Se and Ag-Si-Te systems have been described in literature quite well. The T-x-y diagram of the Ag-Si-Se system is given in [36] and shows that the Ag_8SiSe_6 ternary compound forms in the system, which melts congruently. However, different authors report sharply different values of its melting point. It was shown that it melts at 1203 K in [36, 37], 1258 K in [38], and 1268 K in [39]. The polymorphic transition temperatures of this compound are 315 and 354 K [40]. The low-temperature modificati-

on has tetragonal (Sp.gr. I-4m2, a = 0.7706, b =1.10141 nm) [36, 37], the medium-temperature modification has simple cubic (Sp.gr. P4232, a = 1.087 nm) [41] and high-temperature modification has a face-centered cubic structure (F-43m, a = 1.09413 nm) [36, 37]. The T-x-y diagram of the Ag-Si-Te system shows the formation of Ag_8SiTe_6 ternary compound in the system [37]. This compound has phase transitions at lower temperatures which are 195 K and 263 K[42]. The γ-Ag_8SiTe_6 modification is stable from room temperature to melting temperature and melts congruently at 1143 K [42]. The Ag_8SiTe_6 compound has a cubic structure (Sp.gr.F43m) and the crystal lattice parameter are a =11.5225(7) Å [42], 11.538 Å [43].

MATERIAL AND METHODS

For the thermodynamic study of silver-silicon selenide (telluride), we assembled concentration cell

$$(–)\ Ag\ (s)/Ag_4RbI_5(s)/(Ag\ in\ melt)\ (s)\ (+) \qquad (1)$$

Here, the solid superionic conductor Ag_4RbI_5, which has high ionic conductivity at room temperature, was taken as the electrolyte. In addition, the electron conductivity of this electrolyte is negligible: 10^{-9} S cm^{-1} [44]. Ag_4RbI_5 solid electrolyte was synthesized by the methods described in [45, 46]. During the synthesis, chemically pure AgJ and RbJ compounds were taken and melted in a quartz ampoule under vacuum (10^{-2} Pa) conditions. The alloy was rapidly cooled to room temperature to obtain fine-grained and microscopically homogeneous crystals. Then it was annealed at 400 K temperature for 200 hours to get homogenized ingot. The synthesized compound Ag_4RbI_5 was checked by DTA and XRD methods. During the analysis of this compound, it was observed that it melts with decomposition according to the peritectic reaction at 505 K and crystallizes in the cubic lattice (space group $P4_132$, a = 1.1238 nm), which agreed well with the literature data [44]. Pellets with a diameter of ~1 cm and a thickness of 4-6 mm were cut from the obtained cylindrical ingot and used as a solid electrolyte in cell of type (1). Ag_4RbI_5 solid electrolyte samples prepared by this method were previously successfully used in thermodynamic studies by the EMF method [26-35]. For EMF measurements, silver metal was selected as the left electrode in the solid-state electrochemical cell, and alloys from the Ag_2Se-$SiSe_2$-Se and Ag_2Te-Si_2Te_3-Te composition ranges of the Ag-Si-Se(Te) system were selected as the right electrode (Figure 1). The XRD results of some of the points shown in Figure 1 are shown in Figure 2. As can be seen, in the diffraction pattern of alloy #1, the diffraction lines of Ag_8SiSe_6, $SiSe_2$, and elemental selenium are observed. The diffraction pattern of alloy #3 consists of the sum of the diffraction lines of Ag_8SiTe_6, Si_2Te_3, and elemental tellurium. The composition, synthesis, and thermal annealing conditions of the electrodes taken for both systems are based on the information about the Ag-Si-Se(Te) phase diagrams [36, 37]. The synthesis was carried out by melting stoichiometric mixtures of the corresponding elements with high purity in quartz ampoules under vacuum conditions (10^{-2}Pa). Since the saturated vapor pressure of selenium (T_{boil}=958 K) at the melting temperature of the compounds is high, their synthesis was carried out in a two-zone inclined furnace. The temperature of the furnace was gradually heated to a temperature of 40-50 K above the melting point of the synthesized compound. The obtained melted non-homogenized samples were subjected to prolonged stepwise thermal annealing at 800 K (500 h) and 450 K (200 h).To prepare proper electrodes, the annealed alloys were first powdered and then molded into pellets of 0.5-1 g mass and used as anodes in the solidification cycle.

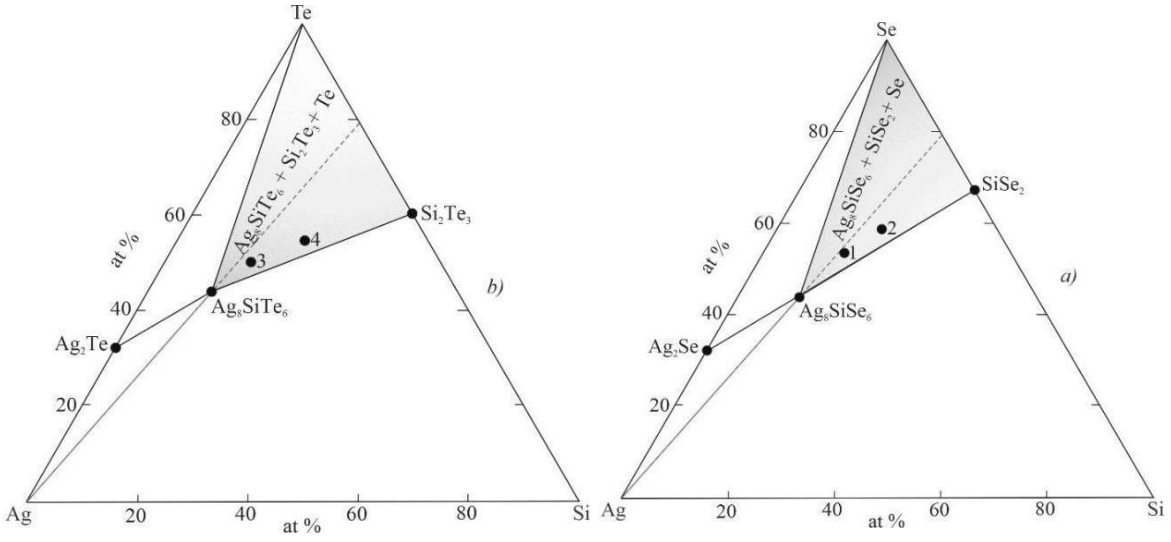

Fig. 1. Solid phase equilibrium diagram at 300 K of the (a) Ag_2Se-$SiSe_2$-Se composition area in the Ag-Si-Se system and (b) Ag_2Te-Si_2Te_3-Te composition area of the Ag-Si-Te system.

A vacuum was created in the concentration cell prepared as given in [45, 46], and it was filled with argon and placed in a specially prepared tube. Here it was kept under thermal control at ~380 K for 40-50 hours. The temperature of the cell was measured with an accuracy of ±0.5°C using chromel-alumel thermocouples and a mercury thermometer. EMF values were measured using a high-resistance digital voltmeter (V7-34A) in the range 360-450K and 300-450 K for both selenide and telluride systems, respectively. After the keeping cell under the conditions mentioned above, the first equilibrium values were recorded and subsequent values were obtained every 3 hours after a given temperature. Equilibrium values were calculated as EMF did not differ by more than 0.5 mV during several measurements at a certain temperature, regardless of the direction of temperature change.

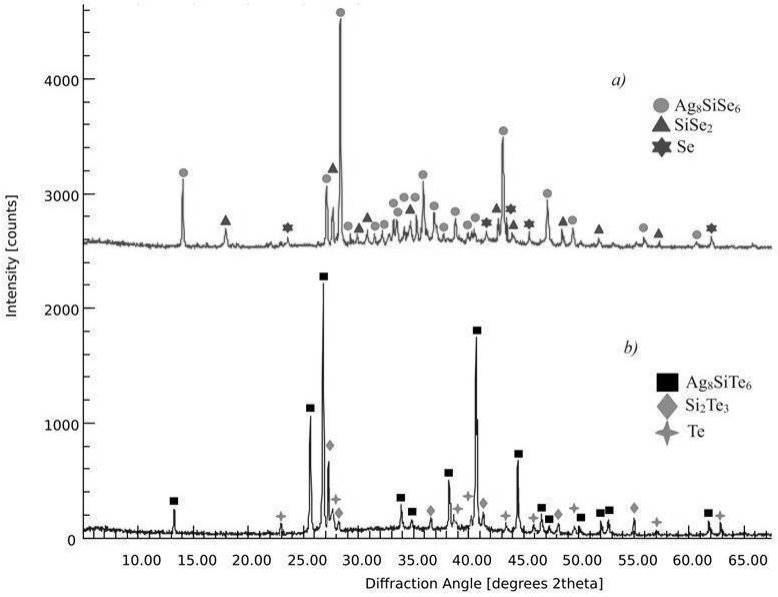

Fig. 2. Powder diffraction patterns of the Ag_2Se-$SiSe_2$-Se and Ag_2Te-Si_2Te_3-Te alloys which shown in Figure 1: (a) alloy #1, (b) alloy #3

RESULTS AND DISCUSSION

Temperature dependences of EMF of type (1) cell are given in Fig. 3. As can be seen, this dependence is linear in the entire temperature range during the measurements for electrode alloys taken from Ag_8SiTe_6+Si_2Te_3+Te phase field. Similarly, a linear dependence was observed in the temperature range of 360-450 K for alloys from the Ag_8SiSe_6+$GeSe_2$+Se phase field. The reproducibility of EMF values in the temperature range of 300-355 K was very low. This can be explained by the fact that the Ag_8SiSe_6 compound undergoes 2 polymorphic phase transitions in that temperature range [40] that are 315 and 354 K. It is possible that there may be kinetic inhibition in these transitions and the samples may not reach equilibrium during the measurements. At 360 K and higher temperatures, the Ag_8SiSe_6 compound is in the high-temperature cubic modification (HT), and the measurements correctly reflect the equilibrium.

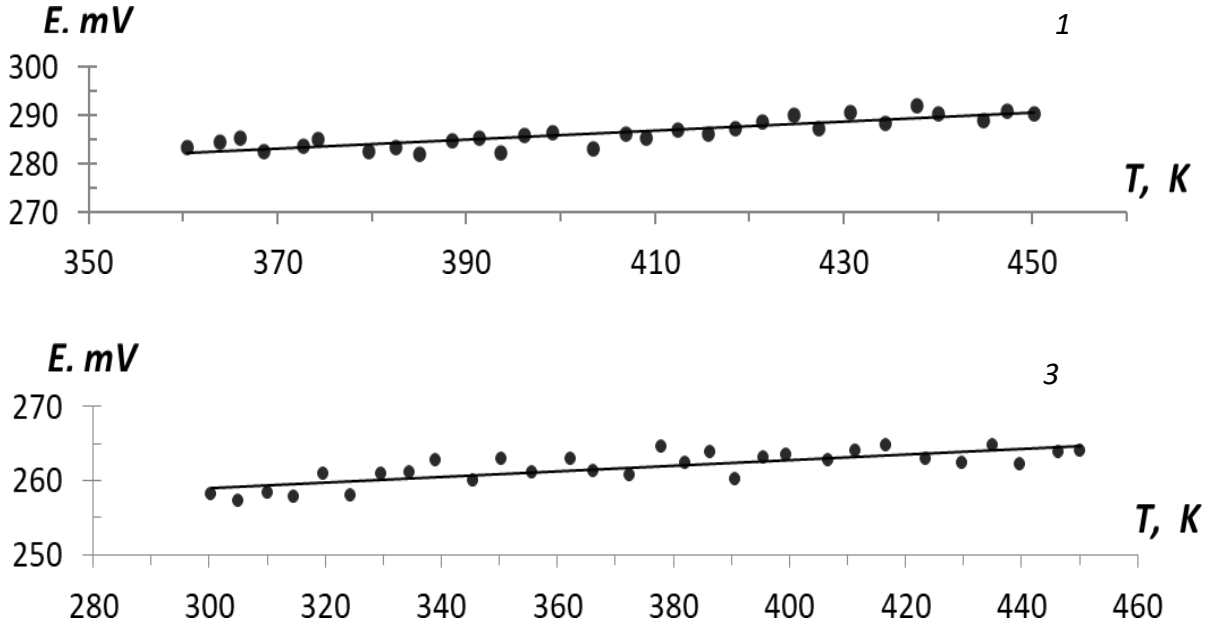

Fig. 3. Temperature dependence of the EMF of concentration cell (1) in the composition area of Ag_2Se-$SiSe_2$-Se(alloy (1) in fig.1) and Ag_2Te-Si_2Te_3-Te(alloy (3) in figure 1), respectively.

Taking into account the mentioned, the results of EMF measurements were processed in the temperature range of 300-450 K for the telluride system and 360-450 K for the selenide system using the least squares method based on a special computer program and linear equations of type (2) were obtained.

$$E = a + bT \pm t\left[\frac{S_E^2}{n} + \frac{S_E^2(T-\bar{T})^2}{\sum(T_i-\bar{T})^2}\right]^{\frac{1}{2}} \quad (2)$$

The results of calculations for HT-Ag_8SiSe_6 is shown in Table 1, and for Ag_8SiTe_6 in Table 2. The obtained equations (2) are presented in Table 3.

Table 1.

Experimentally obtained data for temperature (T_i,), EMF (E_i) and data associated with the calculation steps for the HT-Ag_8SiSe_6.

T_i, K	E_i, mV	$T_i - \bar{T}$	$E_i (T_i - \bar{T})$	$(T_i - \bar{T})^2$	$\tilde{E}$	$E_i - \tilde{E}$	$(E_i - \tilde{E})^2$
360.4	283.29	-44.49	-12603.57	1979.36	282.20	1.09	1.18
363.9	284.55	-40.99	-11663.70	1680.18	282.52	2.03	4.11
366.5	285.21	-38.89	-11091.82	1512.43	282.72	2.49	6.22
368.6	282.59	-36.29	-10255.19	1316.96	282.95	-0.36	0.13
372.7	283.6	-32.19	-9129.08	1036.20	283.33	0.27	0.07
374.3	284.87	-30.59	-8714.17	935.75	283.48	1.39	1.94
379.7	282.49	-25.19	-7115.92	634.54	283.97	-1.48	2.20
382.6	283.33	-22.29	-6315.43	496.84	284.24	-0.91	0.83
385.1	281.84	-19.79	-5577.61	391.64	284.47	-2.63	6.91
388.5	284.68	-16.39	-4665.91	268.63	284.78	-0.10	0.01
391.4	285.36	-13.49	-3849.51	181.98	285.05	0.31	0.10
393.7	282.15	-11.19	-3157.26	125.22	285.26	-3.11	9.66
396.2	285.97	-8.69	-2485.08	75.52	285.49	0.48	0.23
399.1	286.52	-5.79	-1658.95	33.52	285.75	0.77	0.59
403.4	283.11	-1.49	-421.83	2.22	286.15	-3.04	9.23
406.9	286.03	2.01	574.92	4.04	286.47	-0.44	0.19
409.1	285.38	4.21	1201.45	17.72	286.67	-1.29	1.66
412.4	286.99	7.51	2155.29	56.40	286.97	0.02	0.00
415.6	286.05	10.71	3063.60	114.70	287.27	-1.22	1.48
418.5	287.37	13.61	3911.11	185.23	287.53	-0.16	0.03
421.4	288.63	16.51	4765.28	272.58	287.80	0.83	0.69
424.7	289.99	19.81	5744.70	392.44	288.10	1.89	3.57
427.3	287.36	22.41	6439.74	502.21	288.34	-0.98	0.96
430.7	290.67	25.81	7502.19	666.16	288.65	2.02	4.07
434.4	288.39	29.51	8510.39	870.84	288.99	-0.60	0.36
437.8	292.03	32.91	9610.71	1083.07	289.30	2.73	7.44
440.3	290.23	35.11	10189.98	1232.71	289.50	0.73	0.53
444.8	288.83	39.91	11527.21	1592.81	289.95	-1.12	1.24
447.3	290.84	42.41	12334.52	1798.61	290.17	0.67	0.44
450.2	290.17	45.31	13147.60	2053.00	290.44	-0.27	0.07
$\bar{T}$=404,89	=286,284		=1973,65	=21513,51			Σ=66,14

As it is known, the linearity of the dependence of E~f(T) makes it possible to calculate thermodynamic functions using below given expressions below.

$$\Delta\bar{G}_{Ag} = -zFE, \tag{3}$$

$$\Delta\bar{H}_{Ag} = -Z\left[E - T\left(\frac{\partial E}{\partial T}\right)_p\right] = -zFa, \tag{4}$$

$$\Delta\bar{S}_{Ag} = zF\left(\frac{\partial E}{\partial T}\right)_p = zFb \tag{5}$$

Table 2.

Experimentally obtained data for temperature (T_i,), EMF (E_i) and data associated with the calculation steps for the Ag_8SiSe_6.

T_i, K	E_i, mV	$T_i - \bar{T}$	$E_i (T_i - \bar{T})$	$(T_i - \bar{T})^2$	$\tilde{E}$	$E_i - \tilde{E}$	$(E_i - \tilde{E})^2$
300.4	240.29	-73.62	-17690.15	5419.90	239.34	0.95	0.90
304.9	239.55	-69.12	-16557.70	4777.57	239.72	-0.17	0.03
310	238.21	-64.02	-15250.20	4098.56	240.14	-1.93	3.73
314.6	239.59	-59.42	-14236.44	3530.74	240.53	-0.94	0.88
319.7	241.6	-54.32	-13123.71	2950.66	240.95	0.65	0.42
324.3	242.87	-49.72	-12075.50	2472.08	241.34	1.53	2.36
329.7	239.49	-44.32	-10614.20	1964.26	241.79	-2.30	5.27
334.6	242.33	-39.42	-9552.65	1553.94	242.19	0.14	0.02
339.1	243.84	-34.92	-8514.89	1219.41	242.57	1.27	1.61
345.5	244.68	-28.52	-6978.27	813.39	243.10	1.58	2.48
350.4	245.36	-23.62	-5795.40	557.90	243.51	1.85	3.41
355.7	242.15	-18.32	-4436.19	335.62	243.96	-1.81	3.26
362.2	245.97	-11.82	-2907.37	139.71	244.50	1.47	2.17
366.1	246.52	-7.92	-1952.44	62.73	244.82	1.70	2.88
372.4	243.11	-1.62	-393.84	2.62	245.35	-2.24	5.01
377.9	242.03	3.88	939.08	15.05	245.81	-3.78	14.27
382.1	245.38	8.08	1982.67	65.29	246.16	-0.78	0.61
386.4	246.99	12.38	3057.74	153.26	246.52	0.47	0.22
390.6	246.05	16.58	4079.51	274.90	246.87	-0.82	0.67
395.5	247.37	21.48	5313.51	461.39	247.28	0.09	0.01
399.4	248.63	25.38	6310.23	644.14	247.60	1.03	1.06
406.7	249.99	32.68	8169.67	1067.98	248.21	1.78	3.17
411.3	247.36	37.28	9221.58	1389.80	248.59	-1.23	1.52
416.7	250.67	42.68	10698.60	1821.58	249.05	1.62	2.64
423.4	251.39	49.38	12413.64	2438.38	249.60	1.79	3.19
429.8	252.03	55.78	14058.23	3111.41	250.14	1.89	3.58
435	249.23	60.98	15198.05	3718.56	250.57	-1.34	1.80
439.8	248.83	65.78	16368.04	4327.01	250.97	-2.14	4.59
446.3	252.84	72.28	18275.28	5224.40	251.52	1.32	1.76
450.1	250.17	76.08	19032.93	5788.17	251.83	-1.66	2.76
$\bar{T}$=374,02	$\bar{E}$=261,796		$\sum$=2296,53	$\sum$=60400,43			$\sum$=55,63

Partial molar thermodynamic functions of silver in alloys were calculated based on equations (3)-(5) (Table 4). Since the HT-Ag_8SiSe_6 phase is not stable under standard conditions, its partial Gibbs free energy was also calculated for 400 K temperature.

Table 3.

Equations of the temperature dependence of EMF of type (1) cell in some phase fields of Ag-Si-Se(Te) systems

Phase field	E, mV = a+bt±tS_E(T)
β-Ag_8SiSe_6 + $SiSe_2$ + Se	$249{,}14 + 0{,}0917T \pm 2\left[\frac{2{,}2}{30} + 1{,}1 \cdot 10^{-4}(T - 404{,}9)^2\right]^{\frac{1}{2}}$
Ag_8SiTe_6 + Si_2Te_3 + Te	$247{,}58 + 0{,}0380T \pm 2\left[\frac{1{,}9}{30} + 3{,}1 \cdot 10^{-5}(T - 374{,}0)^2\right]^{\frac{1}{2}}$

As can be seen from the fragments of the solid phase equilibrium diagrams of Ag-Si-Se(Te) systems (Figure 1), the tie-lines starting from the Ag corner of Gibbs triangle and passing through the stoichiometric compositions of Ag_8SiSe_6 and Ag_8SiTe_6 compounds, respectively and enters Ag_8SiSe_6 + $SiSe_2$ + Se and Ag_8SiTe_6 + Si_2Te_3 + Te three-phase fields. That is, the phase diagrams show that under equilibrium conditions (imaginary) Ag removal from the compound Ag_8SiSe_6 would lead to $SiSe_2$ and elemental Se. Similarly, when Ag was removed from Ag_8SiTe_6, a mixture of Si_2Te_3 + Te would be obtained. It is seen that according to the solid-phase equilibrium diagram (Fig. 1), the values of the relative partial molar functions are a response to the following virtual-cell reactions:

$$8Ag + SiSe_2 + 4Se = Ag_8SiSe_6 \quad (6)$$

$$8Ag + 0{,}5Si_2Te_3 + 4{,}5Te = Ag_8SiTe_6 \quad (7)$$

Therefore, the integral thermodynamic functions of ternary compounds were calculated from the expressions given below: (Δ Z≡ Δ G, Δ H)

$$\Delta_f Z^o(Ag_8SiSe_6) = 8\Delta\bar{z}_{Ag} + \Delta_f Z^o(SiSe_2) \quad (8)$$

$$\Delta_f Z^o(Ag_8SiTe_6) = 8\Delta\bar{z}_{Ag} + 0{,}5\Delta_f Z^o(Si_2Te_3) \quad (9)$$

Absolute entropies can be calculated based on the expressions:

$$S^o(Ag_8SiSe_6) = 8[\Delta\bar{S}_{Ag} + S^o(Ag)] + S^o(SiSe_2) + 4S^o(Se) \quad (10)$$

$$S^o(Ag_8SiTe_6) = 8[\Delta\bar{S}_{Ag} + S^o(Ag)] + 0{,}5S^o(Si_2Te_3) + 4{,}5S^o(Te) \quad (11)$$

The results of calculations according to equations (8)-(11) are given in Table 5. The errors were calculated by the error accumulation method. During the calculation of integral thermodynamic functions, in addition to the quantities obtained by the EMF method (Table 4), the standard entropies of the elementary components involved in reactions (6) and (7) taken from the database (Ag-42.55±0.13 J(K) ·mol)), as well as the thermodynamic functions of $SiSe_2$ and Si_2Te_3 compounds were used. Literature data on the thermodynamic properties of both compounds are contradictory.

Table 4.

Partial thermodynamic functions of silver in alloys of Ag-Si-Se(Te) systems (T=298.15K)

Phase field	$\bar{G}$	$\bar{H}$	$-\Delta\bar{S}_{Ag}$, J·mol^{-1}·K^{-1}
	kJ·mol^{-1}		
β-Ag_8SiSe_6 + $SiSe_2$ + Se	26,68±0,11 *27,58±0,11	24,04±0,40	8,85±0,98
Ag_8SiTe_6 + Si_2Te_3 + Te	24,98±0,05	23,89±0,20	3,67±0,53

Comparative analysis of the obtained values for enthalpy of formation of $SiSe_2$ compound in different works [47, 49-52] are discussed in [48] and values very close to the calorimetric results obtained by O'Hare et al. [49] were recommended (Table 5). The results given in different sources [48-51] for the Si_2Te_3 compound are also quite different. We used the values of melting enthalpies and absolute entropies of these compounds given in [46, 50], as well as the calculated standard Gibbs energies of formation using these quantities (Table 5).

Table 5.

Integral thermodynamic functions of HT-Ag_8SiSe_6 and Ag_8SiTe_6 compounds with some relevant literature data for $SiSe_2$ and Si_2Te_3 compounds

Compound	$-\Delta_fG^o$	$-\Delta_fH^o$	Δ_fS^o	S^o
	kJ·mol^{-1}		kJ·mol^{-1}·K^{-1}	
SiSe2	175,3±3,5 - -	177,6±3,2[46] 178,4±3,1[47] 208±57[48]	- - -	95,2±2.0[52] - -
Si2Te3	70,9±10	65±10[48] 76,6±10[50] 71±10[51] 80±15[49]		167,0±3,0[52]
β-Ag8SiSe6	388,7±4,4	369,9±6,4	63,1±9,8	675±12
Ag8SiTe6	235,3±5,4	229,4±6,6	19,8±9,2	676±11

CONCLUSION

In the present paper, we report the results of a thermodynamic study of the Ag_2Se-$SiSe_2$-Se and Ag_2Te-Si_2Te_3-Te subsystem using the EMF method with an Ag_4RbI_5 solid electrolyte in a temperature range from 360 to 450 K and from 300 to 450, respectively. According to the EMF measurements, the partial molar functions of silver in two-phase regions, β-Ag_8SiSe_6 + $SiSe_2$ + Se and Ag_8SiTe_6 + Si_2Te_3 + Te at 298 K, as well as the standard thermodynamic functions of the formation and standard entropies of β-Ag_8SiSe_6 and Ag_8SiTe_6, were calculated. Since the HT-

Ag_8SiSe_6 phase is not stable under standard conditions, its partial Gibbs free energy was also calculated for 400 K temperature.

REFERENCES

1. Babanly, M.B. Ternary Chalcogenides Based on Copper and Silver (Тройные халькогениды на основе серебра и меди) / M.B.Babanly, Y.A.Yusibov, V.T. Abishev – Russia: BSU Publisher, – 1993. – 342 p.
2. Chalcogenides: From 3D to 2D and Beyond / X.L.Sanghoon, L.J.Tengfei, L.Y. Zhang [et al.] – Elsevier, – 2019. – 398 p.
3. Ahluwalia, G.K. Applications of Chalcogenides: S, Se, and Te / G.K. Ahluwalia. – Springer, – 2016. – 461 p.
4. Schwarzmüller, S. Argyrodite-Type Cu_8GeSe_6-xTe_x($0 \leq x \leq 2$): Temperature-Dependent Crystal Structure and Thermoelectric Properties // Zeitschrift Für Anorganische Und Allgemeine Chemie, – 2018. №24, – p. 1915-1922.
5. Acharya, S. High thermoelectric power factor in p-type Cu_8GeSe_6 // Solid-state physics symposium, – 2019. – p. 1-3.
6. Li, W. Low Sound Velocity Contributing to the High Thermoelectric Performance of Ag_8SnSe_6 / W. Li, S. Lin, B. Ge [et al.] // Advanced Science, – 2016. №11, – p. 1600196-1600201.
7. Ghrib, T. High Thermoelectric Figure of Merit of Ag_8SnS_6 Component Prepared by Electrodeposition Technique / T. Ghrib, A.L. Otaibi, A. Almessiere [et al.] // Chinese Physics Letters, – 2015. №12, – p. 127402-127409.
8. Jin, M. Fabrication and Thermoelectric Properties of Single-Crystal Argyrodite Ag_8SnSe_6 / M. Jin, S. Lin, W. Li [et al.] // Chemistry of Materials, – 2019. №7, – p. 2603-2610.
9. Shen, X. High-Temperature Structural and Thermoelectric Study of Argyrodite Ag_8GeSe_6 / X. Shen, C. Yang, Y. Liu [et al.] // ACS Applied Materials and Interfaces, – 2019. №2, – p. 2168-2176.
10. Charoenphakdee, A. Ag_8SiTe_6: A New Thermoelectric Material with Low Thermal Conductivity // A. Charoenphakdee, K. Kurosaki, H. Muta [et al.] // Japanese Journal of Applied Physics, – 2009. №1, – p. 01160-01169.
11. Qinghui, J. Eco-friendly Highly Robust Ag_8SiSe_6-Based Thermoelectric Composites with Excellent Performance Near Room Temperature / J. Qinghui, L.Suwei, L.Yubo [et al.] // ACS publications, – 2020. №49, – p. 54653-54661.
12. Masaki, F. Thermoelectric properties of Ag_8GeTe_6 / F. Masaki, K. Ken, M. Hiroaki [et al.] // Journal of Alloys and Compounds, – 2005. №1, – p. 280-282.
13. Semkiv, I. Ag_8SnSe_6 argyrodite synthesis and optical properties / I. Semkiv, H. Ilchuk, M. Pawlowski [et al.] // Opto-Electronics Review, – 2017. №1, – p. 37-40.
14. Lu, C.L. Electronic, optical properties, surface energies and work functions of Ag_8SnS_6: First-principles method / C.L. Lu, L. Zhang, Y.W. Zhang [et al.] // Chinese Physics B, – 2015. №1, – p. 1-7.
15. Boon-on, P. Ag_8SnS_6: a new IR solar absorber material with a near -optimal bandgap / P. Boon-on, B. A. Aragaw, C.Y. Shi [et al.] // Royal Society of chemistry Advances, – 2018. №8, – p.39470-39476.
16. Brammertz, G. Fabrication and characterization of ternary Cu_8SiS_6 and Cu_8SiSe_6 thin film layers for optoelectronic applications / G. Brammertz, B.Vermang, H. ElAnzeery [et al.] // Thin Solid Films, – 2016. №616, – p. 649-654.
17. Somnath, A. Enhancement of Power Factor for Inherently Poor Thermal Conductor Ag_8GeSe_6 by Replacing Ge with Sn / A. Somnath, J. Pandey, A. Soni [et al.] // American Chemical Society Applied Energy Materials, – 2019. №2, – p. 654-660.
18. Hull, S. Ag^+ diffusion within the rock-salt structured superionic conductor $Ag_4Sn_3S_8$ // Journal

of Physics Condensed Matter, – 2005. №7, – p. 1067-1084.
19. Barbara, K.H. High Electron Mobility and Disorder Induced by Silver Ion Migration Lead to Good Thermoelectric Performance in the Argyrodite Ag_8SiSe_6 / K.H. Barbara, W. Kai, K.Yasar [et al.] // Materials Science and Engineering, – 2017. – p. 4833-4839.
20. Boucher, F. Distribution and Ionic Diffusion Path of Silver in γ-Ag_8GeTe_6: A Temperature Dependent Anharmonic Single Crystal Structure Study / F. Boucher, M. Evain, R. Brec // Journal of Solid State Chemistry, – 1993. №2, – p. 332-346.
21. Ashirov, G.M. Ionic conductivity of the Ag_8GeSe_6 compound / G.M. Ashirov, R.M. Sardarly, L.F. Mashadiyeva [et al.] // Modern Physics Letters B, – 2023. – p. 32-34.
22. West, D.R. Ternary Phase Diagrams in Materials Science / D.R.West. CRC Press, – 2019. – 236 p.
23. Hiroyasu, S. Introduction To Phase Diagrams In Materials Science And Engineering / S. Hiroyasu. World Scientific Publishing Company, – 2020. – 188 p.
24. Babanly, M.B. Some issues of complex investigation of the phase equilibria and thermodynamic properties of the ternary chalcogenide systems by the EMF method / M.B. Babanly, L.F. Mashadiyeva, D.M. Babanly [et al.] // Russian Journal of Inorganic Chemistry, – 2019. №13, – p. 1649-1671.
25. Imamaliyeva, S.Z. Physicochemical Aspects of Development of Multicomponent Chalcogenide Phases Having the Tl_5Te_3 Structure: A Review / S.Z. Imamaliyeva, D.M. Babanly, D.B. Tagiev [et al.] // Russian Journal of Inorganic Chemistry, – 2018. №13, – p.1703-1730.
26. Aspiala, M. Thermodynamic study in the Ag–Sb–S system by the EMF method / M. Aspiala, F. Tesfaye, and P. Taskinen [et al.] // The Journal of Chemical Thermodynamics, – 2016. – p. 361-368.
27. Babanly, N.B. Thermodynamic investigation of silver-thallium tellurides by EMF method with solid electrolyte Ag_4RbI_5 / N.B. Babanly, E.N. Orujlu, S.Z. Imamaliyeva [et al.] // The Journal of Chemical Thermodynamics, – 2019. – p. 78-88.
28. Babanly, N.B. Thermodynamic study of the Ag–Tl–Se system using the EMF method with Ag_4RbI_5 as a solid electrolyte / N.B. Babanly, S.Z. Imamaliyeva, Y.A. Yusibov [et al.] // Journal of solid state electrochemistry, – 2018. – p. 1143-1149.
29. Mashadieva, L.F. Thermodynamic study of the $2PbTe–AgSbTe_2$ system using EMF technique with the Ag_4RbI_5 solid electrolyte / L.F. Mashadieva, S.G. Mansimova, Y.A. Yusibov [et al.] // Russian Journal of Electrochemistry, – 2018. – p. 106-112.
30. Babanly, M.B. Phase diagram and thermodynamic properties of compounds of the AgI–TlI–I system / M.B. Babanly, L.F. Mashadieva, Z.S.Aliev [et al.] // Journal of Alloys Compound, – 2012. – p. 38-48.
31. Mashadieva, L.F. Experimental investigation of the Ag–Bi–I ternary system and thermodynamic properties of the ternary phases / L.F. Mashadieva, Z.S. Aliev, A.V. Shevelkov [et al.] // Journal of Alloys Compound, – 2013. – p. 512-518.
32. Mashadiyeva, L.F. The $Ag_2Te–SnTe–Bi_2Te_3$ system and thermodynamic properties of the $(2SnTe)_1 – x(AgBiTe_2)_x$ solid solutions series / L.F. Mashadiyeva, J.O. Kevser, I.I. Aliev [et al.] // Journal of Alloys Compound, – 2017. – p. 641-648.
33. Mashadiyeva, L.F. Phase Equilibria in the $Ag_2Te–SnTe–Sb_2Te_3$ System and Thermodynamic Properties of the $(2SnTe)_{12x}(AgSbTe_2)_x$ Solid Solution/ L.F. Mashadiyeva, J.O. Kevser, I.I. Aliev [et al.] // Journal of Phase Equilibria and Diffusion, – 2017. – p. 603.
34. Alverdiev, I. Thermodynamic study of Ag_8GeSe_6 by EMF with an Ag_4RbI_5 solid electrolyte / I. Alverdiev , S.M. Bagkheri, S.Z. Imamalieva [et al.] // Russian Journal of Electrochemistry, – 2017. – p. 551.
35. Babanly, M.B. Thermodynamic study of the Ag–As–Se and Ag–S–I systems using the EMF method with a solid Ag_4RbI_5 electrolyte / M.B. Babanly, L.F. Mashadiyeva, G.M. Veliyeva, [et al.] // Russian Journal of Electrochemistry, – 2015. – p. 399.

36. Hofmann, A.M. Silver-Selenium-Silicon // Ternary Alloys, – 1988. – p. 559-560.
37. Gorochov, O. Les composés $A_{g8}MX_6$ (M= Si, Ge, Sn et X= S, Se, Te) // Bulletin de la Société Chimique de France, – 1968. №101, – p. 2263-2275.
38. Venkatraman, M. The phase diagrams of M_2X -SiX_2 (M is Cu, Ag; X is S, Se) / M. Venkatraman, R. Blachnik, A. Schlieper [et al.] // Thermochimica Acta, – 1995. №249, – p. 13-20.
39. Piskach, L.V. Interaction of argyrodite family compounds with the chalcogenides of II-b elements / L.V. Piskach, O.V. Parasyuk, I.D. Olekseyuk [et al.] // Journal of Alloys and Compounds, – 2006. №421, – p. 98-104.
40. Amiraslanova, A.J. Phase equilibria in the Ag_8SiSe_6- Ag_8SiTe_6 system and characterization of solid solutions $Ag_8SiSe_{6-x}Te_x$ / A.J. Amiraslanova, K.N. Babanly, S.Z. Imamaliyeva [et al.] // Applied Chemical Engineering, – 2023. – p. 48-53.
41. Heep, B.K. High electron mobility and disorder induced by silver ion migration lead to good thermoelectric performance in the argyrodite Ag_8SiSe_6 / B.K. Heep, K.S. Weldert, Y. Krysiak [et al.] // Chemistry of Materials, – 2017. №29, – p. 4833-4839.
42. Boucher, F. Single-crystal structure determination of γ-Ag_8SiTe_6 and powder X-ray study of low-temperature α and β phases / F. Boucher, M. Evain and R. Brec // Journal of Solid State Chemistry, – 1992. – p. 341-355.
43. Charoenphakdee, A. Ag_8SiTe_6: A New Thermoelectric Material with Low Thermal Conductivity / A. Charoenphakdee, K. Kurosaki, H. Muta [et al.] // Japanese Journal of Applied Physics, – 2009. – p. 011603.
44. Ivanov-Shchits, A.K., Murin I.V. Ionika tverdogo tela // Solid State Ionics, – 2000. – p. 462-466.
45. Babanly, M.B. Elektrokhimicheskie metody v termodinamike neorganicheskikh sistem (Electrochemical Methods in Thermodynamics of Inorganic Systems) / M.B. Babanly, Yu.A. Yusibov – Baku: Elm, – 2011.
46. Olin, A. Chemical thermodynamics of selenium / A. Olin, N.G. Evgeny – France: 2005, –851p.
47. Tomaszkiewicz, I. Fluorine-combustion calorimetric determinations of the standard molar enthalpy changes for the formation of $SiSe_2$(cr), $SiSe_{1.94}$(cr), and $SiSe_{1.94}$(vit), and for the transition: $SiSe_{1.94}$(vit) = $SiSe_{1.94}$(cr) at the temperature T = 298.15 K. Implications of the results for the enthalpies of dissociation Dom(Se–SiSe) and Dom(SiSe). Thermodynamic properties of SiSe(g) / I. Tomaszkiewicz, S. Susman, K. Volin [et al.] // The Journal of ChemicalThermodynamics,– 1994.№10,–p.1081-1093
48. Chandrasekharaiah, D.S. Continuum Mechanics / D.S. Chandrasekharaiah, L. Debnath – 1994. – 595p.
49. O'Hare, P.A.G. Termodynamic proporties of $SiSe_2$ // Journal of Chemistry Thermodynamics, – 1986.
50. Exsteen, G. Enthalpies of Formation of Solid Silicon Dichalcogenides / G. Exsteen, J. Drowart, A. Vander [et al.] // Journal of Physics and Chemistry, – 1966. №12, – p. 4130-4131.
51. Brebrick, R.F. Thermodynamic study of silicon sesquitelluride using a mass spectrometer / R.F.Brebrick,–1968.
52. Materials Thermochemistry / O.Kubaschewski [et al.]. – Oxford: Pergamon, – 1993. – 363 p.

GÜMÜŞ-SİLİSİUM SELENİDLƏRİN (TELLURİDLƏRİN) EMF METODU İLƏ AG_4RBI_5 BƏRK ELEKTROLİT İSTİFADƏSİ İLƏ TERMODİNAMİK TƏDQİQİ

G.M. Əşirov, K.N. Babanlı, L.F. Məşədiyeva

Ag-Si-Se sisteminin Ag_2Se-$SiSe_2$-Se altsistemi EHQ(elektrik hərəkət qüvvəsi) üsulu ilə 360-450K temperatur intervalında, Ag-Si-Te sisteminin Ag_2Te-Si_2Te_3-Te altsistemi isə 300-450K

temperature intervalında Ag_4RbI_5 bərk elektroliti ilə öyrənilmişdir. Hər iki sistem üzrə hazırlanmış nümunələrdə EHQ-nin temperaturdan asılılığının xətti olduğu müşahidə edilmişdir. Ag-Si-Se(Te) sistemlərinin xəlitələrində gümüşün parsial termodinamik funksiyaları hesablanmışdır. Eyni zamanda hər iki sistemdə yaranan üçlü birləşmələrin (Ag_8SiSe_6, Ag_8SiTe_6) standart inteqral termodinamik funsksiyaları hesablanmışdır. β-Ag_8SiSe_6 üçün Δ_fG dəyəri həm standart hal üçün həm də 400K- üçün hesablanmışdır.

Açar sözlər: *gümüş-silisum selenidləri,telluridləri, faza keçidləri, termodinamik funksiyalar, EHQ üsulu, Ag_4RbI_5 bərk elektrolidi*

ТЕРМОДИНАМИЧЕСКОЕ ИССЛЕДОВАНИЕ СИВЕР-СЕЛЕНИДОВ (ТЕЛЛУРИДОВ) КРЕМНИЯ МЕТОДОМ ЭДС С ТВЕРДЫМ ЭЛЕКТРОЛИТОМ AG_4RBI_5

Г.М. Аширов, К.Н. Бабанли, Л.Ф. Машадиева

Подсистема Ag_2Se-$SiSe_2$-Se системы Ag-Si-Se исследована в интервале температур 360-450 К, а подсистема Ag_2Te-Si_2Te_3-Te системы Ag-Si-Te - в диапазоне 300-450 К. температурный диапазон методом ЭДС (электродвижущей силы) с твердым электролитом Ag_4RbI_5. Было замечено, что зависимость ЭДС от температуры была линейной в образцах, приготовленных для обеих систем. По результатам измерений ЭДС рассчитаны парциальные термодинамические функции серебра в сплавах систем Ag-Si-Se(Te), а также стандартные интегральные термодинамические функции тройных соединений Ag_8SiSe_6 и Ag_8SiTe_6. Кроме того, были рассчитаны стандартные интегральные термодинамические функции β-Ag_8SiSe_6 как в стандартных условиях, так и при 400 К.

Ключевые слова: *селениды серебра–кремния, теллуриды, фазовый переход, термодинамические функции, метод ЭДС, твердый электролит Ag_4RbI_5*